


ORIGINAL ARTICLE

A jacalin-like lectin domain-containing protein of *Sclerospora graminicola* acts as an apoplastic virulence effector in plant–oomycete interactions

Michie Kobayashi¹  | Hiroe Utsushi¹ | Koki Fujisaki¹ | Takumi Takeda¹ | Tetsuro Yamashita² | Ryohei Terauchi^{1,3}

¹Iwate Biotechnology Research Center, Kitakami, Iwate, Japan

²Iwate University, Morioka, Iwate, Japan

³Laboratory of Crop Evolution, Graduate School of Agriculture, Kyoto University, Muko, Kyoto, Japan

Correspondence

Michie Kobayashi, Iwate Biotechnology Research Center, Kitakami, Iwate, Japan. Email: kobayashim856@affrc.go.jp

Present address

Michie Kobayashi, Institute of Agrobiological Sciences, National Agriculture and Food Research Organization (NARO), Tsukuba, Ibaraki, Japan

Funding information

Japan Society for the Promotion of Science, Grant/Award Number: KAKENHI/19K06062

Abstract

The plant extracellular space, including the apoplast and plasma membrane, is the initial site of plant–pathogen interactions. Pathogens deliver numerous secreted proteins, called effectors, into this region to suppress plant immunity and establish infection. Downy mildew caused by the oomycete pathogen *Sclerospora graminicola* (Sg) is an economically important disease of Poaceae crops including foxtail millet (*Setaria italica*). We previously reported the genome sequence of Sg and showed that the jacalin-related lectin (JRL) gene family has significantly expanded in this lineage. However, the biological functions of JRL proteins remained unknown. Here, we show that JRL from Sg (SgJRL) functions as an apoplastic virulence effector. We identified eight SgJRLs by protein mass spectrometry analysis of extracellular fluid from Sg-inoculated foxtail millet leaves. SgJRLs consist of a jacalin-like lectin domain and an N-terminal putative secretion signal; SgJRL expression is induced by Sg infection. Heterologous expression of three SgJRLs with N-terminal secretion signal peptides in *Nicotiana benthamiana* enhanced the virulence of the pathogen *Phytophthora palmivora* inoculated onto the same leaves. Of the three SgJRLs, SG06536 fused with green fluorescent protein (GFP) localized to the apoplastic space in *N. benthamiana* leaves. INF1-mediated induction of defence-related genes was suppressed by co-expression of SG06536-GFP. These findings suggest that JRLs are novel apoplastic effectors that contribute to pathogenicity by suppressing plant defence responses.

KEYWORDS

apoplastic effector, downy mildew, foxtail millet, jacalin-related lectin, *Sclerospora graminicola*

1 | INTRODUCTION

To counter the constant attacks by pathogens, plants mount defence responses (Jones & Dangl, 2006). The first battleground of plants and pathogens is the extracellular space, including plant surfaces and the apoplast. Plants release a battery of hydrolases, protease

inhibitors, and antimicrobial compounds into the apoplast to prevent microbial infection (Doehlemann & Hemetsberger, 2013; Wang et al., 2019; Wang & Wang, 2018). Plant proteases and protease inhibitors suppress pathogen growth directly or indirectly (Jashni et al., 2015). In addition, plant β -1,3-glucanase and chitinases degrade major components of the cell walls of fungi and oomycetes. Pattern recognition

This is an open access article under the terms of the [Creative Commons Attribution-NonCommercial-NoDerivs](https://creativecommons.org/licenses/by-nc-nd/4.0/) License, which permits use and distribution in any medium, provided the original work is properly cited, the use is non-commercial and no modifications or adaptations are made.

© 2022 The Authors. *Molecular Plant Pathology* published by British Society for Plant Pathology and John Wiley & Sons Ltd.

receptors localized on the plant cell surface sense elicitor molecules such as pathogen-associated molecular patterns (PAMPs), microbe-associated molecular patterns, and damage-associated molecular patterns and activate immune responses. As a counterdefence, pathogens manipulate plant immune responses using virulence effectors, resulting in successful infection.

Oomycetes (also known as water moulds) are a diverse group of filamentous eukaryotic microorganisms that include saprophytes as well as pathogens of plants, insects, crustaceans, vertebrates, and various microorganisms (Lamour & Kamoun, 2009; Thines & Kamoun, 2010; Wang et al., 2019). More than 60% of known oomycete species are parasitic on plants (Thines & Kamoun, 2010), in which they cause devastating diseases in a wide range of species, including agricultural crops. Oomycetes secrete a series of effectors to manipulate plant physiology and suppress plant immunity (Kamoun, 2006). Whole-genome sequencing and transcriptome analysis of various oomycetes revealed that they share a common set of effectors. These effectors are classified as apoplastic or cytoplasmic based on their localization in the host plant. Apoplastic effectors include secreted hydrolytic enzymes such as proteases, lipases, and glycosylases that can degrade plant tissue, protease inhibitors that protect oomycetes from host defence enzymes, necrosis- and ethylene-inducing peptide 1-like proteins (NLPs), and PcF-like small cysteine-rich proteins (SCRs; Kamoun, 2006). By contrast, RXLR domain-containing proteins and crinklers are cytoplasmic effectors that are specific to plant-pathogenic oomycetes (Morgan & Kamoun, 2007; Torto et al., 2003).

Sclerospora graminicola is an obligate biotrophic oomycete that causes downy mildew disease in Poaceae plants including foxtail millet, pearl millet, and maize. We previously performed whole-genome sequencing of *S. graminicola* and determined that a gene family encoding jacalin-like lectin domain-containing proteins (JRLs) has significantly expanded (Kobayashi et al., 2017). Many SgJRLs have putative secretion signals at their N-termini and their expression is up-regulated during *S. graminicola* infection, suggesting that SgJRLs are novel effectors of *S. graminicola*. However, the functions of SgJRLs remain unknown, primarily due to the difficulty of genetically manipulating oomycetes, including *S. graminicola*.

Here we report that JRLs of *S. graminicola* are indeed secreted into the apoplast. Using the model pathosystem of *Nicotiana benthamiana* and *Phytophthora palmivora*, we show that transient overexpression of SgJRL in the plant enhances *P. palmivora* growth and partially suppresses plant defence responses. These findings indicate that JRL is a novel apoplastic effector that contributes to the virulence of oomycetes.

2 | RESULTS

2.1 | *S. graminicola* delivers JRLs into the plant apoplast during early infection

To investigate the molecular mechanisms underlying plant–microbe interactions in the apoplastic space during *S. graminicola* infection, we extracted extracellular fluid (EF) from *S. graminicola*-inoculated

foxtail millet leaves at 1 and 3 days postinoculation (dpi). We then compared the proteins contained in the EF to those of the soluble fraction (SF) from total leaf homogenates. Thaumatin-like protein, an apoplastic marker protein, was detected by anti-thaumatin antibodies in the EF but not in the SF, whereas FBPase, a cytoplasmic marker detected by anti-FBPase antibodies, was abundant in the SF but not in the EF (Figure S1), indicating that apoplastic proteins were considerably enriched in our EF preparation. Therefore, we subjected the EF proteins to mass spectrometry (MS) analysis (Figure S2). Liquid chromatography coupled with tandem MS (LC-MS/MS) analysis identified 75 *S. graminicola* proteins, including 19 putative secreted proteins (Table S1). Most putative secreted proteins were contained in the low-molecular-weight fraction from leaves at 3 dpi (Table S1, fractions 3dpi-3 to 3dpi-5). Therefore, we performed another experiment focusing on the low-molecular-weight fractions, which identified 23 *S. graminicola* proteins, including 10 putative secreted proteins (Table S2). Seven putative secreted proteins were common to the first and second experiments (Table 1, shaded).

Combining the two experiments, a total of 22 proteins were identified as putative apoplastic secreted proteins, including eight JRLs, four NLPs, one arabinofuranosidase, one protease inhibitor, and one transglutaminase elicitor, among others (Table 1). Phylogenetic analysis and amino acid sequence alignment of the SgJRLs showed that the eight JRLs are not similar to each other among SgJRL family members, but all contained a jacalin domain with conserved amino acid residues (Figure 1, Figure S3). All eight JRL genes were induced during *S. graminicola* infection, with their highest expression at 2 dpi (Figure 2). These data indicate that JRLs are candidate apoplastic effectors with possible roles in virulence during the early infection stage (c.2 dpi). Therefore, we focused on the JRLs in subsequent analysis.

2.2 | JRLs with secretion signals promote *P. palmivora* infection in *N. benthamiana* leaves

Because genetic manipulation of foxtail millet and *S. graminicola* is difficult, we used a model system consisting of *N. benthamiana* and *P. palmivora* to evaluate the possible virulence functions of JRLs. To investigate the functions of SgJRLs in the apoplast, we replaced their predicted secretion signal peptides with that of *Nicotiana tabacum* PR1a (NtPR1a; GenBank accession X06930.1; Figure 3a). Because the NtPR1a signal peptide is highly effective at targeting proteins to the apoplast via the endoplasmic reticulum (ER)/Golgi secretory pathway in solanaceous plants (Hammond-Kosack et al., 1994), we expected that SgJRLs with the NtPR1a signal peptide would accumulate in the apoplast. To test the effects of JRL expression, we transiently expressed eight JRLs (designated SG02945, SG03255, SG04896, SG05109, SG05127, SG06536, SG10124, and SG17166 in this study) with or without the NtPR1a signal peptide in *N. benthamiana* leaves and inoculated the same leaves with *P. palmivora* 2 days after agro-infiltration. At 3 dpi, transient expression of the three proteins SG03255, SG06536, and SG17166 with

TABLE 1 Putative secreted proteins of *Sclerospora graminicola* identified in the extracellular fluid of *S. graminicola*-inoculated foxtail millet leaves

| Accession | Mass | Description | Exp_1 ^a | Exp_2 ^a |
|----------------------|---------|---|--------------------|--------------------|
| SG14735 | 35,549 | Arabinofuranosidase | ✓ | |
| SG08752 | 49,348 | Calreticulin precursor | ✓ | |
| SG02395 | 50,987 | Exonuclease | ✓ | |
| SG14267 | 61,637 | Glucose-methanol-choline oxidoreductase | ✓ | |
| SG02945 ^b | 19,042 | JRL | ✓ | ✓ |
| SG03255 ^b | 16,328 | JRL | ✓ | ✓ |
| SG04896 | 18,357 | JRL | | ✓ |
| SG05109 ^b | 19,699 | JRL | ✓ | ✓ |
| SG05127 | 18,563 | JRL | ✓ | |
| SG06536 ^b | 16,412 | JRL | ✓ | ✓ |
| SG10124 ^b | 17,422 | JRL | ✓ | ✓ |
| SG17166 ^b | 18,094 | JRL | ✓ | ✓ |
| SG00344 | 26,908 | NLP | ✓ | |
| SG05755 ^b | 29,163 | NLP | ✓ | ✓ |
| SG10403 | 27,419 | NLP | ✓ | |
| SG14292 | 26,664 | NLP | | ✓ |
| SG05676 | 9,704 | Phospholipase D | ✓ | |
| SG14096 | 13,994 | Protease inhibitor | ✓ | |
| SG18945 | 640,765 | Protocadherin fat-like protein | ✓ | |
| SG12053 | 45,595 | Transglutaminase elicitor | ✓ | |
| SG00883 | 22,153 | Uncharacterized | ✓ | |
| SG03074 | 18,464 | Uncharacterized | | ✓ |

JRL, jacalin-like lectin domain-containing protein; NLP, necrosis- and ethylene-inducing peptide 1-like protein.

^aExp_1 and Exp_2 indicate proteins identified in the first and second experiments, respectively.

^bProteins identified in both experiments.

FIGURE 1 Amino acid sequence alignment of the jacalin-like lectin domain consensus sequence (jacalin domain) and SgJRLs without the N-terminal signal sequence. Multiple sequence alignment was performed using ClustalW and illustrated by BOXSHADE (https://embnet.vital-it.ch/software/BOX_form.html). Identical amino acids are shaded in black, and similar amino acids are shaded in grey. Orange shading indicates peptides identified by liquid chromatography–mass spectrometry analysis

| | | |
|----------------|-----|--|
| Jacalin-domain | 1 | -----GVRKVVYVGGEDGIAYIKFEYVK |
| SG05109 | 1 | ---TFSQDAGMVPDMNICGSAKGDVYFNDLILNSDMTYPSFWIQGDKRVSIVASAFPTT |
| SG05127 | 1 | -----QDSFVNEGKVFGNPNSKVNFDKGDILPGIKLPSAWGGDERVTVGVLQYVMP |
| SG02945 | 1 | QBYQGVPPLQIQYGKKFGD-RSVNTVSDDEQIFNGAKVPAVAHQDGDLDGPAIYYG- |
| SG10124 | 1 | -----DSFDDTKAATKAIADKRTPPYAWHGVRNDRVTCFGIHYG |
| SG06536 | 1 | -----TTDFDPAFDHMTVKRFHIWAD-SNQVYGVQVDVNE |
| SG17166 | 1 | -----EDGDFSGEGRSDSNVSVSDGTEVVRVYIYEDNQRVVGVIWDP |
| SG04896 | 1 | -----QRGISTKYFGKKPDSDLAAVYPTMNVLSISVQGINERVIGVSLTYKT |
| SG03255 | 1 | -----TFPFGD-DQKAAGLQLLSIDLHYGDRIVIGVGLNFEX |
| Jacalin-domain | 24 | AGGKVEGDEHCKKGLLCTEEFELDYPDEYITSTVECTYDKVPSSESEVFTSIRKFKTKNGRT |
| SG05109 | 58 | IP-SNEKYPHC--VDTCRKTTLTGGDKRIVQSNVTCYAD-----DTGYSMLKFRSNPDFV |
| SG05127 | 54 | DG-RQCKFEHC--IKGCAES--KIEDEEHLVAVKCNFD-----SEGIVVLEFRNIVHSSK |
| SG02945 | 59 | ----DKKNAHC--PYKQOYSPVTVGNDREVVVQTCVLD-----GSCVHYLEFRNIVHPTK |
| SG10124 | 40 | ---ADRSFDHCDQGDKDDSSKNIHKKPEDRIRISVLLTSD-----SKGITVVEFRVMLSGV |
| SG06536 | 37 | AG-KDQNAFHC--TSQCFEKVLSLEKGRHITRFMKTST-----EGKVLRLLSGPNQV |
| SG17166 | 45 | ---LKLVPVHC--ESPCHAQSLQSLGDEYIIGGEISVV-----RQDVIYVLEFRNIVKPGN |
| SG04896 | 49 | LEGGVSSLRHC--FVDSKAQSMNIGTGEHIMSI FGVGN-----GDGTYIGFAFRKQGV |
| SG03255 | 36 | ---EVGVFHC--HKTCTFQSNKVDVDRGEYITGFSAYLD-----SNSKRVHLSLNRGKN |
| Jacalin-domain | 84 | SELFGTKS-----GTFKSLEEKEGKKRIVGPHCRAGNLLNALGA----- |
| SG05109 | 109 | NKNSIEVG--TLPDPVPSDIEHVAPEGHQGGFRGVVGNNGGITDQLLWVSIK |
| SG05127 | 103 | GVRSIHGG--KVPD-NPNSIPHELKAAVHLVGFPTCTVVDSGFPRRAMLWVDD----- |
| SG02945 | 107 | APISAGAKPAQITEAMKEKAPDATFIKHQLGFPISGERDGIKIVPETIIVVVVN----- |
| SG10124 | 91 | VLNSIMAG-----KQNGKPTPILEDCKHVLGFPSCGVDDNGLKSLTVLWTPDK |
| SG06536 | 88 | IDAGMMGG-----NPSPEHPDCKQLGFPSCGVVAGNGDADSALLKIFPVVVAI- |
| SG17166 | 94 | SVAVGRKD-----PTATIPFSQPRNTDQVGFPEGVVGDGILREINVIWCKTRDCT- |
| SG04896 | 101 | ISAGKKPP-----AMTPEMYDNRTATYQVGFPAFAVEGNILKAGAYWACIDANDCS |
| SG03255 | 84 | SLVFGNSQ-----AMYPNPQAAPSGLQVGFCTGQNNNDYVTDIGPVVGGQP |

signal peptides resulted in larger disease lesion sizes than transient expression of their counterpart proteins lacking signal peptides (Figure 3b). Expressed SG03255, SG06536, and SG17166 proteins of the predicted sizes were detected by immunoblot analysis (Figure 3c). These results suggest that JRL proteins SG03255, SG06536, and SG17166 are secreted into the apoplast and have virulence functions that enhance *P. palmivora* growth in planta.

2.3 | SP-SG06536-GFP localizes to the apoplast in *N. benthamiana* leaves

To validate the localization of the SgJRLs to the apoplast, we fused green fluorescent protein (GFP) to the C-terminus of each SgJRL with or without the secretion signal from NtPR1a (PR1aSP-SgJRL-GFP and ΔSP-SgJRL-GFP, respectively; Figure 4a, Figure S4a). We then transiently

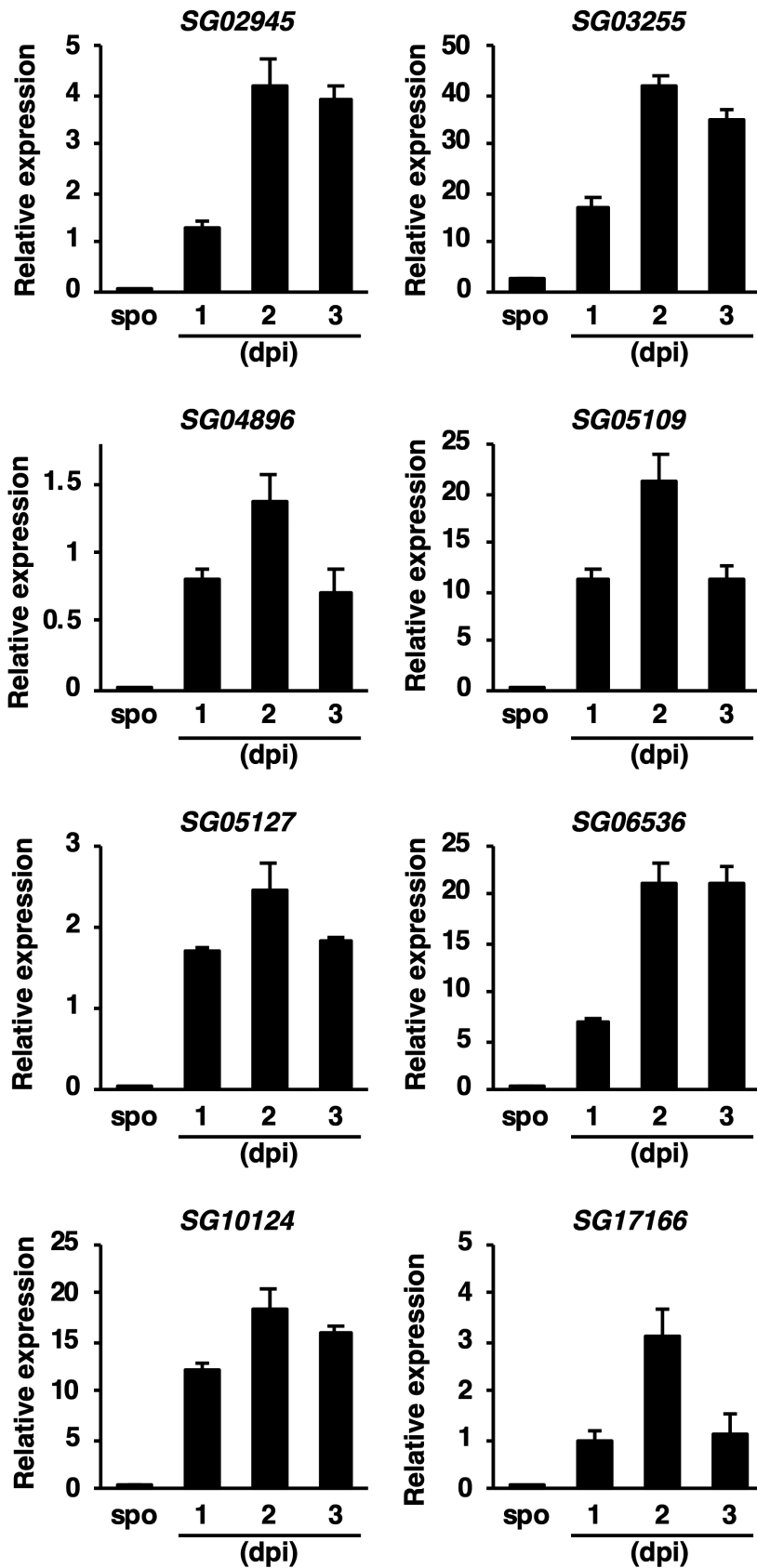


FIGURE 2 Relative expression levels of genes encoding jacalin-like lectin domain-containing proteins identified in the extracellular fluid from foxtail millet leaves inoculated with *Sclerospora graminicola*. *Histone H2A* was used as a reference gene for normalization. spo, *S. graminicola* conidiospores; dpi, days postinoculation. $n = 3$

expressed the PR1aSP-SgJRL-GFP and Δ SP-SgJRL-GFP fusion proteins in *N. benthamiana* leaves and visualized them by confocal microscopy. By combined plasmolysis and FM4-64 staining, we detected the

accumulation of PR1aSP-SgJRL-GFP in the apoplastic space, while the Δ SP-SgJRL-GFP proteins and the control (GFP) remained in the cytoplasm, except for SG17166 (Figure 4b, Figures S4b and S5). These

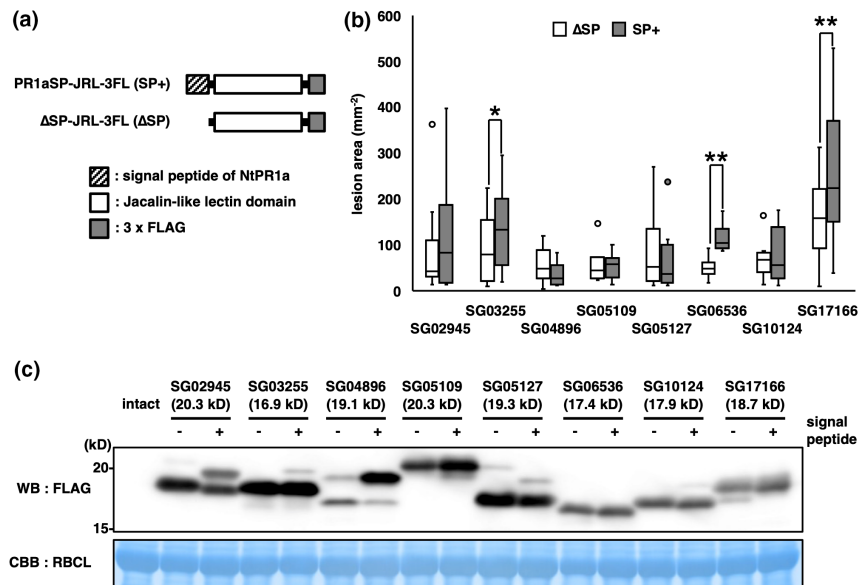


FIGURE 3 Jacalin-like lectin domain-containing proteins (JRLs) with secretion signals promote *Phytophthora palmivora* infection in *Nicotiana benthamiana* leaves. (a) Diagrams of SgJRL and the fusion proteins used in this study. (b) JRLs with or without the secretion signal sequence (SP) from NtPR1a were transiently expressed in *N. benthamiana* leaves. Two days after agro-infiltration, the leaves were detached and inoculated with *P. palmivora*. Lesion area was measured at 3 days postinoculation. Asterisks indicate significant differences ($*p < 0.05$, $**p < 0.01$, $n = 8-12$) using the paired two-tailed Student's *t* test. Boxplot centre lines show the medians; box limits indicate the 25th and 75th percentiles; whiskers extend 1.5 times the interquartile range from the 25th and 75th percentiles; outliers are represented by dots. (c) Leaves expressing JRLs were sampled 2 days after agro-infiltration, and proteins were detected using anti-FLAG antibodies by western blotting (WB). Protein loads were monitored by Coomassie brilliant blue (CBB) staining of the bands corresponding to ribulose-1,5-bisphosphate carboxylase large subunit (RBCL). Intact indicates nonagro-infiltration control

observations confirm the translocation of PR1aSP-SgJRL-GFP to the region outside the cells and imply that it functions in the apoplast.

Of the JRLs examined, the effect of SG06536 on *P. palmivora* growth showed the clearest difference in the presence versus the absence of the signal peptide (Figure 3b). Therefore, we evaluated the growth of *P. palmivora* in *N. benthamiana* overexpressing SG06536-GFP. Compared to GFP, PR1aSP-SG06536-GFP but not ΔSP-SG06536-GFP promoted the spread of *P. palmivora* disease lesions in *N. benthamiana* (Figure 4c,d). In addition, the biomass of *P. palmivora* was correlated with the sizes of the disease lesions (Figure 4e). Transiently expressed PR1aSP-SG06536-GFP and ΔSP-SG06536-GFP proteins accumulated to similar levels in *N. benthamiana* leaves, as determined by immunoblot analysis (Figure S6). These data are consistent with the results above (Figure 3b) and highlight the importance of the secretion of SG06536 into the apoplast to support *P. palmivora* infection.

2.4 | SG06536 expression inhibits PAMP-triggered responses

To investigate the effects of SG06536 on plant defence responses, we examined the expression of defence-related genes *PAL* and *RBOHB*. INF1 is a PAMP derived from *Phytophthora* species (Kamoun et al., 1997) that induces plant defence responses. In agro-infiltrated leaves, *PAL* expression was induced and reached a peak at 9 h after treatment, and *RBOHB* expression increased until

12 h after treatment (Figure S7). We then infiltrated INF1 peptides into *N. benthamiana* leaves expressing GFP, PR1aSP-SG06536-GFP, and ΔSP-SG06536-GFP at 2 days after agro-infiltration. At 9 h after INF1 treatment, the expression levels of *PAL* and *RBOHB* were lower in PR1aSP-SG06536-GFP-expressing leaves than in GFP- and ΔSP-SG06536-GFP-expressing leaves (Figure 5). PR1aSP-SG06536-GFP-expression had no effect on the timing or levels of INF1-induced cell death (Figure S8). These results suggest that SG06536 in the apoplastic space suppresses PAMP-triggered responses.

3 | DISCUSSION

In this study, we investigated *S. graminicola* proteins in the host apoplast. Although the purity of the apoplastic fraction is often a concern in the analysis of apoplastic proteins, the EF produced in this study appeared to be significantly enriched with apoplastic proteins, as demonstrated by immunoblot analysis of thaumatin-like protein, an apoplastic marker (Figure S1). Supporting this notion, LC-MS/MS analysis identified several plant apoplastic proteins in the EF, including PR proteins with higher scores than in the SF (Tables S4 and S5). We also identified several *S. graminicola* apoplastic effector candidates in the EF (Tables S1 and S2). NLPs are widespread effectors among filamentous and bacterial pathogens. In oomycetes, two types of NLPs (type 1 [cytotoxic] and type 1a [noncytotoxic]) have been reported (Oome & Ackerveken, 2014). The SgNLPs identified in this study are type 1a NLPs; such NLPs

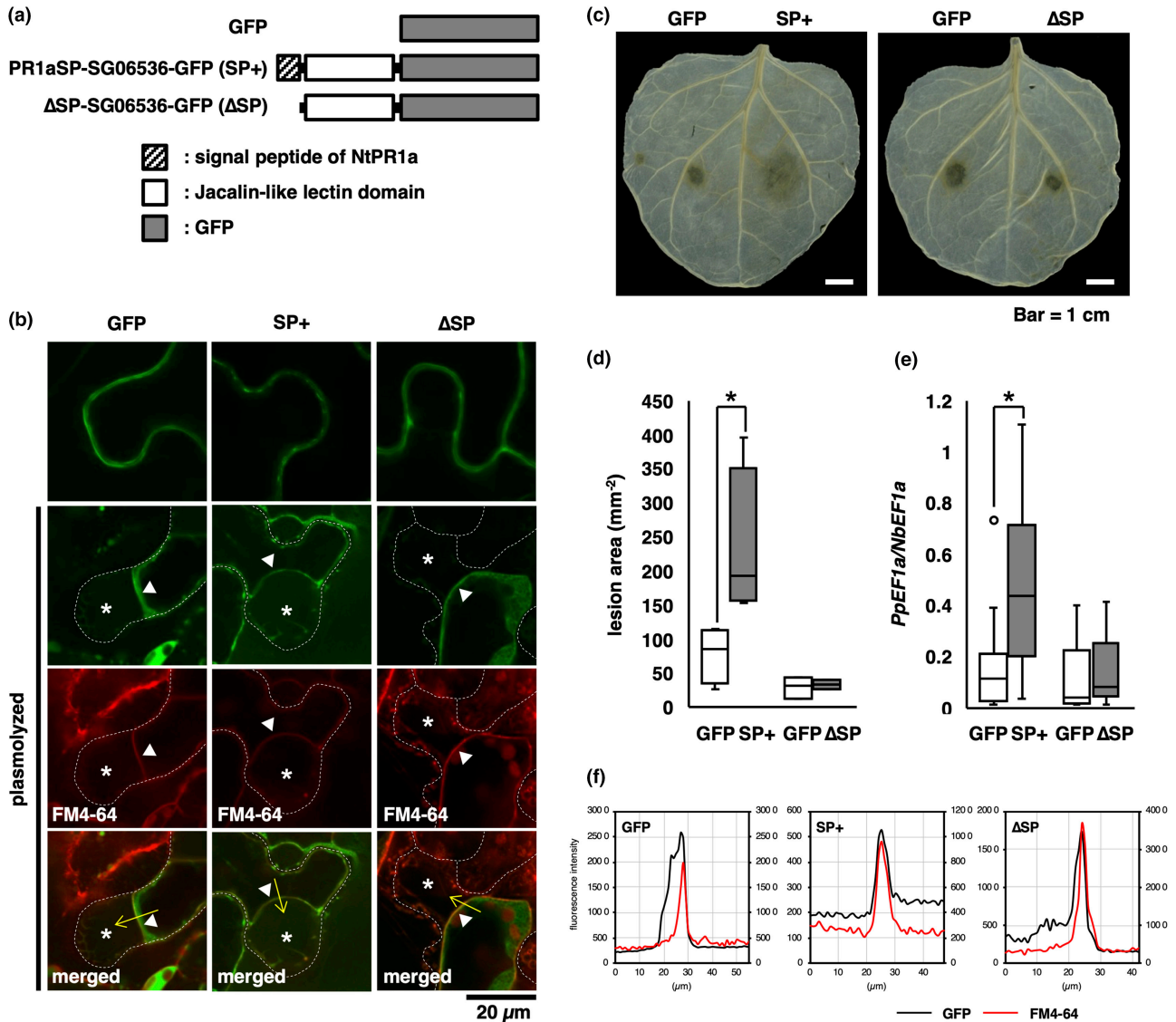


FIGURE 4 SG06536 with a signal peptide (SP) accumulates in the plant apoplast. (a) Diagrams of SG06536 and the fusion proteins used in this study. (b) Genes were transiently expressed in *Nicotiana benthamiana* leaves. The leaves were examined 3 days after agro-infiltration. In plasmolyzed cells, the dashed white line marks the cell wall, asterisks indicate the apoplastic space, and triangles indicate the position of the plasma membrane. Yellow arrows represent transects depicted in (f) and Figure S5. Bar = 20 μ m. (c) SG06536 with or without the secretion signal sequence from NtPR1a was transiently expressed in *N. benthamiana* leaves. Two days after agro-infiltration, the leaves were detached and inoculated with *Phytophthora palmivora*. The leaves were decoloured and photographed at 3 days postinoculation (dpi). (d) Lesion area was measured at 3 dpi. Asterisk indicates a significant difference ($p < 0.05$, $n = 4$) using the paired two-tailed Student's *t* test. (e) The ratio of *P. palmivora* to *N. benthamiana* biomass assayed by quantitative PCR using DNA isolated from leaves at 3 dpi. Asterisk indicates a significant difference ($p < 0.05$, $n = 18$) using the paired two-tailed Student's *t* test. (d, e) Boxplot centre lines show the medians; box limits indicate the 25th and 75th percentiles; whiskers extend 1.5 times the interquartile range from the 25th and 75th percentiles; outliers are represented by dots. (f) Fluorescence intensity plots of transect through cells expressing green fluorescent protein (GFP) or GFP fusion proteins. The left y axis is fluorescence intensity of GFP, the right y axis is fluorescence intensity of FM4-64, and the x axis is the distance from the starting point of the yellow arrow in (b)

are thought to play a role in the biotrophic phase of oomycete infection (Oome & Ackerveken, 2014), but the details of their function remain unclear. Further analysis of SgNLPs will be required to understand the infection strategy of *S. graminicola*.

In the current study, we focused on SgJRLs, because the SgJRL gene family appears to have undergone a unique expansion process in *S. graminicola* that did not occur in related oomycetes (Kobayashi

et al., 2017). The *S. graminicola* genome encodes 45 JRLs with putative N-terminal secretion signals. Eight of these proteins were identified in our LC-MS/MS analysis in the current study. All eight SgJRLs were highly expressed during the early phase of *S. graminicola* infection, which is in agreement with their abundance detected by MS analysis (Figure 2, Tables S1 and S3). Three of these eight (SG03255, SG06536, and SG17166) promoted *P. palmivora* infection

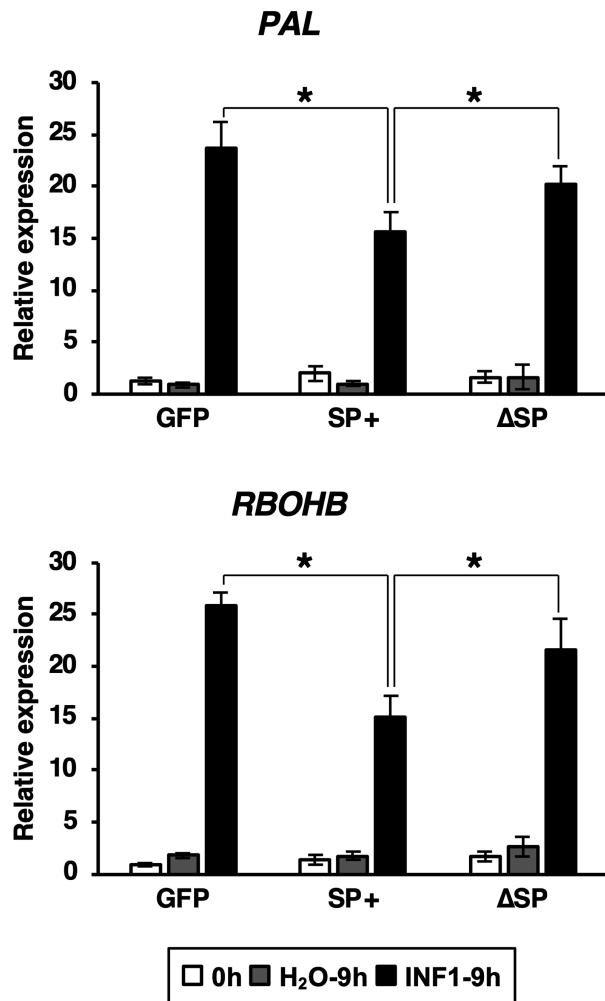


FIGURE 5 INF1-mediated induction of *PAL* and *RBOHB* in *Nicotiana benthamiana* leaves is partially suppressed by the expression of SP-SG06536-GFP. Two days after agroinfiltration, the leaves were subjected to INF1 treatment. The relative expression levels were analysed by reverse transcription quantitative PCR, with *NbEF1a* used as a reference gene for normalization. *p* values were calculated using Dunnett's multiple-comparisons test. Asterisk indicates a significant difference ($p < 0.05$, $n = 3$)

in *N. benthamiana* leaves (Figure 3b). Because both expression levels in foxtail millet leaves (Figure 2) and protein accumulation levels in *N. benthamiana* leaves (Figure 3c) were not correlated with pathogenicity, their pathogenicity is thought to be due to the protein function. Phylogenetic analysis and amino acid sequence alignment of the SgJRLs showed that the three JRLs are not similar to each other among SgJRL family members (Figure 1; Figure S3). Therefore, we cannot infer the functions of JRLs based on their primary sequences. Determining the three-dimensional structures of the SgJRLs would be useful for elucidating their functions in the future (de Guillen et al., 2015; Win et al., 2012).

In this study, we used the signal peptide of NtPR1a to deliver SgJRL to the plant apoplast, and identified three effector candidates. Furthermore, we analysed the three effector candidates with native

signal peptides as well (Figures S9 and S10). Consistent with the effects of SgJRLs with the NtPR1a signal peptide, the three SgJRLs with their native signal peptides tended to enhance *P. palmivora* pathogenicity (Figure S9). However, quantitative effects of the effectors on oomycete pathogenicity were different from those of the effectors with the NtPR1a signal peptide (Table S8). Because the effector candidates with either NtPR1a or native signal peptides seem to be translocated to the apoplast (Figure 4B, Figures S4 and S10), we currently cannot explain this differential effect. Figure S9 shows that SG03255 with its native signal peptide significantly affected *P. palmivora* pathogenicity. Therefore, in addition to the effector functions in foxtail millet, SG03255 with its native signal peptide in *N. benthamiana* will also be analysed in future work.

JRLs were previously identified as candidate effectors based on genome analysis of *Phytophthora infestans* (Raffaele et al., 2010). However, the functions of JRLs in filamentous pathogens are not known. JRLs are lectins that reversibly bind to carbohydrates such as mannose and galactose. Several pathogen carbohydrate-binding proteins function as virulence effectors in the apoplast. For example, the LysM domain-containing proteins Ecp6, Slp1, and Mg3LysM prevent chitin-triggered plant immunity by binding to chitin oligosaccharides (de Jonge et al., 2010; Marshall et al., 2011; Mentlak et al., 2012). Mg1LysM, Mg3LysM, and Avr4 protect fungal hyphae against plant-derived hydrolytic enzymes, probably by binding to the fungal cell wall (van den Burg et al., 2006; Marshall et al., 2011). The fungi-specific β -glucan-binding lectin FGB1 alters fungal cell wall composition to protect against plant hydrolases, and it also suppresses β -glucan-triggered immunity (Wawra et al., 2016). All of these factors contribute to fungal pathogenicity by binding to carbohydrates derived from fungal cell walls. We have not yet successfully detected the binding of SgJRLs to the cell walls of either oomycetes or foxtail millet. NLPs, which have structural similarities to fungal lectins, bind to glycosylinositol phosphorylceramide, a major lipid of the plant plasma membrane, and causes necrosis in eudicots (Lenarčič et al., 2017; Ottmann et al., 2009). These observations point to possible roles of JRLs in the apoplast.

In the current study, we identified three JRLs (SG03255, SG06536, and SG17166) that affect *P. palmivora* infection in *N. benthamiana*, two of which (PR1aSP-SG03255-GFP and PR1aSP-SG06536-GFP) accumulate in the apoplastic space, whereas PR1aSP-SG17166-GFP was not visibly localized to the apoplast (Figure S4). We also demonstrated that PR1aSP-SG06536-GFP expression has an inhibitory effect on plant defence responses (Figure 5). These data suggest that at least the secreted protein SG06536 supports *P. palmivora* infection and suppresses plant defence responses in the apoplast.

In contrast to JRLs from pathogens, information is available about the roles of plant JRLs in disease resistance (Esch & Schaffrath, 2017). TaJRL1, a wheat JRL, is induced by biotic and abiotic stimuli and is thought to be a component of salicylic acid- and jasmonic acid-dependent defence signalling (Xiang et al., 2011). Overexpression of OsJAC1 confers quantitative broad-spectrum resistance against fungal, oomycete, and bacterial pathogens in rice (*Oryza sativa*; Weidenbach et al., 2016). Although they are likely to be intracellular

proteins, some host JRLs can function in the apoplast: for example, rice OsMBL1. Overexpression of *OsMBL1* induces resistance to rice blast (caused by *Magnaporthe oryzae*), whereas MoChi1, an *M. oryzae* chitinase, inhibits the resistance response by competing with OsMBL1 for chitin (Han et al., 2019). Therefore, it is possible that SgJRLs mimic or compete with host JRLs that function in the apoplast.

We demonstrated that an SgJRL functions as a novel virulence effector. Genome analysis showed that oomycetes closely related to *S. graminicola* have JRLs, whereas *Pythium* spp., oomycetes distantly related to *S. graminicola*, and other fungi, such as *M. oryzae* and *Colletotrichum graminicola*, do not have low-molecular-weight JRLs with signal peptides encoded in their genomes (Table S6). Notably, *S. graminicola* has a uniquely expanded JRL family among related oomycetes (Kobayashi et al., 2017). Among the oomycetes with available genome sequences, only *S. graminicola* infects monocots. Therefore, perhaps the expansion of the JRL family represents an adaptation of this pathogen to monocots. The differential functions of JRLs in monocots and dicots are of great interest and should be clarified in the future.

4 | EXPERIMENTAL PROCEDURES

4.1 | Plant and oomycete materials and inoculation

Foxtail millet (*Setaria italica* 'Ootsuchi-10'), obtained with permission from the experimental field of the Iwate Agricultural Research Center, Karumai, Iwate, Japan, was used in this study. A strain of *S. graminicola* isolated from a single zoospore was derived from an isolate collected with permission from the Iwate Agricultural Research Center field in 2013. The plants were grown in an artificial climate chamber at 20–25°C under a 15 h light/9 h dark cycle. Four-week-old plants were infected with *S. graminicola* by spraying them with a mixture of sporangia and zoospores ($1-5 \times 10^5$ per ml). Seven days after inoculation, the leaves were harvested, rinsed with distilled water, and used to prepare the inoculum. Sporulation was induced by incubating the infected leaves at 100% humidity at 25°C for 5–6 h. Mixtures of sporangia and zoospores were collected by rinsing the sporulated leaves with chilled sterile water. *N. benthamiana* plants were grown for 4–5 weeks at 25°C under a 16 h light/8 h dark cycle. *P. palmivora* (MAFF 242760) was maintained on rye medium at 25°C. For inoculation, *P. palmivora* was subcultured on V8 medium in the dark for 3 days, followed by 3 days under a 16 h light/8 h dark cycle. The mycelium was suspended in cold water, filtered through Miracloth, and concentrated by centrifugation, and zoospore production was induced at room temperature. Detached *N. benthamiana* leaves were inoculated with 10- μ l aliquots of zoospores (10^5 zoospores/ml) and covered with lens paper (4 mm diameter) to keep the zoospore suspension on the leaf surface. The leaves were kept at high humidity at 25°C.

4.2 | Preparation of the extracellular fluid and soluble protein fractions

Foxtail millet leaves inoculated with *S. graminicola* were harvested and vacuum-infiltrated with 50 mM HEPES-KOH, pH 6.8, for 20 min. The leaf surface was dried, and the leaf material was placed into a 25-ml syringe and inserted into a 50-ml Falcon tube, which was then centrifuged at $1500 \times g$ for 10 min. An aliquot of the sample was immediately mixed with protease inhibitor cocktail. The sample was used as the EF fraction for MS and immunoblot analysis. To extract the soluble protein fraction, the leaves were ground in liquid nitrogen and dissolved in three volumes of GTN extraction buffer (25 mM Tris-HCl, pH 7.0, 150 mM NaCl, 10% glycerol, 10 mM dithiothreitol, and complete protease inhibitor cocktail). The samples were centrifuged at $20,000 \times g$ for 10 min and the supernatant was used as the soluble protein fraction (SF).

4.3 | Mass spectrometry

The proteins were analysed by SDS-PAGE and Coomassie brilliant blue staining (Figures S1 and S2). The protein bands were excised from the gel, treated with trypsin, and analysed by MS using an LTQ Orbitrap XL mass spectrometer (Thermo Fisher Scientific, Inc.) as described previously (Takahashi et al., 2013).

4.4 | *Agrobacterium tumefaciens*-mediated transient expression (agro-infiltration) in *N. benthamiana*

Binary plasmids were transformed into *A. tumefaciens* GV3101, followed by overnight culture. The culture was diluted 10-fold in Luria-Bertani medium containing kanamycin and rifampicin and cultured until it reached $OD_{600} = 0.6$. The cells were harvested by centrifugation and resuspended in MES/MgCl₂ (10 mM MES-NaOH, pH 5.6, 10 mM MgCl₂, 150 μ M acetosyringone). The suspensions were adjusted to $OD_{600} = 1.0$ and incubated for 1–2 h at room temperature. Bacterial suspensions containing P19, SgJRL, and MES/MgCl₂ were mixed at a 1:5:4 ratio and infiltrated into the leaves of 4- to 5-week-old *N. benthamiana* plants using a needleless syringe. Two or three days after infiltration, the leaves were used for various experiments.

4.5 | Immunoblot analysis

N. benthamiana leaves were ground in liquid nitrogen and dissolved in six volumes of GTN extraction buffer. SDS-PAGE sample buffer was added to the samples, which were then boiled for 5 min, chilled on ice, and centrifuged at $20,000 \times g$ for 10 min to remove debris. Equal volumes of samples were separated on SDS-PAGE gels (e-Pagel; ATTO). Horseradish peroxidase (HRP)-conjugated

monoclonal mouse anti-FLAG produced in mouse clone M2 (Sigma-Aldrich) and anti-GFP pAb-HRP-DirecT (MBL) were used at 1:10,000 dilution to detect FLAG- and GFP-tagged proteins, respectively.

For immunoblot analysis of foxtail millet proteins, the protein concentrations of the SF and EF were determined using Protein Assay Dye Reagent (Bio-Rad) with bovine serum albumin as a standard. Five micrograms of proteins was separated by SDS-PAGE (e-Pagel; ATTO). Anti-cFBPase (AS04 043; Agrisera) was used as the primary antibody at 1:10,000 dilution. To prepare anti-thaumatin-like protein antiserum, the SGQKPLTLAEFTIGGSQ peptide was synthesized and polyclonal antiserum was raised in rabbit (GenScript). HRP-conjugated anti-rabbit IgG (Promega) was used as the secondary antibody at 1:10,000–20,000 dilution. To detect the signals, Chemi-Lumi One (Nacalai Tesque, Inc.) was used as a substrate for HRP, and the signal was visualized using an ImageQuant LAS 4000 system (GE Healthcare Life Sciences).

4.6 | RNA and DNA extraction, quantitative PCR

Total RNA was extracted from the samples using a NucleoSpin RNA Plant kit (Takara Bio Inc.) in accordance with the manufacturer's instructions. The RNA was reverse transcribed into cDNA using PrimeScript (Takara Bio Inc.). Quantitative PCR (qPCR) was performed using Kapa SYBR FAST qPCR Master Mix (Kapa Biosystems; Roche) on a QuantStudio 3 Real-time PCR System (Thermo Fisher Scientific, Inc.). To quantify *P. palmivora* biomass, total DNA was extracted from the samples as follows. Three days postinoculation with *P. palmivora*, leaves (20 mm diameter) were ground in liquid nitrogen, dissolved in 300 μ l of CTAB (3% cetyltrimethylammonium bromide, 100 mM Tris-HCl, pH 8.0, 1.4 M NaCl, 20 mM EDTA), and incubated at 60°C for 30 min. The samples were vortexed by adding chloroform, and the water layer was fractionated by centrifugation. The DNA was precipitated with isopropanol, treated with RNase A, and purified using a QIAquick PCR Purification Kit (Qiagen) in accordance with the manufacturer's instructions. qPCR was performed using Kapa SYBR FAST qPCR Master Mix or Luna Universal qPCR Master Mix (NEB) on a QuantStudio 3 system. The primer sequences are listed in Table S7.

4.7 | Plasmid construction

All primers used in this study are listed in Table S7. To construct plasmids for reverse transcription qPCR and qPCR analysis, cDNA fragments of *SgJRLs*, *SgHistone*, *NbEF1 α* , and *PpEF1 α* were cloned into pCR8/GW/TOPO or pCR-Blunt (Thermo Fisher Scientific, Inc.). To analyse virulence and protein accumulation in *N. benthamiana*, cDNA fragments of the signal peptide of *NtPR1 α* , the *SgJRL* genes, and *GFP* were amplified and cloned into pCambia-C-3 \times FLAG (Maqbool et al., 2015).

4.8 | Confocal laser-scanning microscopy

Agrobacterium suspensions were infiltrated into the leaves of 4- to 5-week-old *N. benthamiana* plants using a needleless syringe. Three days after infiltration, the leaves were observed under a Fluoview FV1000 confocal laser-scanning microscope (Olympus). Plasmolysis was performed by incubating the leaves in 0.75 M mannitol solution. GFP and FM4-64 were excited by a 488-nm laser and detected with bandpass 505–605- and 655–755-nm filters, respectively.

4.9 | Preparation and treatment with the INF1 elicitor

The INF1 elicitor was prepared from *Escherichia coli* DH5 α cells carrying the chimeric plasmid pFB53 containing the *inf1* gene (Kamoun et al., 1997), as previously described (Shibata et al., 2010). *N. benthamiana* leaves were infiltrated with 150 nM (for gene expression analysis) or 1.5 μ M (for cell death analysis) INF1 solution using a needleless syringe.

4.10 | Experimental design

Each experiment was performed at least twice with at least three biological replicates per experiment.

ACKNOWLEDGEMENTS

We thank S. Kamoun of The Sainsbury Laboratory, Norwich, UK, S. Schornack of The Sainsbury Laboratory, Cambridge, UK, and K. Naito of the National Institute of Agrobiological Sciences for their valuable suggestions for improving the manuscript. This work was supported by JSPS KAKENHI grant number 19K06062. We thank the NARO Genebank for providing *P. palmivora*. Computations were partially performed on the NIG supercomputer at the ROIS National Institute of Genetics.

DATA AVAILABILITY STATEMENT

The data that support the findings of this study are available from the corresponding author upon reasonable request.

ORCID

Michie Kobayashi  <https://orcid.org/0000-0003-0277-8978>

REFERENCES

- van den Burg, H.A., Harrison, S.J., Joosten, M.H.A.J., Vervoort, J. & de Wit, P.J.G.M. (2006) *Cladosporium fulvum* Avr4 protects fungal cell walls against hydrolysis by plant chitinases accumulating during infection. *Molecular Plant-Microbe Interactions*, 19, 1420–1430.
- Doehlemann, G. & Hemetsberger, C. (2013) Apoplastic immunity and its suppression by filamentous plant pathogens. *New Phytologist*, 198, 1001–1016.

- Esch, L. & Schaffrath, U. (2017) An update on jacalin-like lectins and their role in plant defense. *International Journal of Molecular Sciences*, 18, 1592.
- de Guillen, K., Ortiz-Vallejo, D., Gracy, J., Fournier, E., Kroj, T. & Padilla, A. (2015) Structure analysis uncovers a highly diverse but structurally conserved effector family in phytopathogenic fungi. *PLoS Pathogens*, 11, e1005228.
- Hammond-Kosack, K.E., Harrison, K. & Jones, J.D.G. (1994) Developmentally regulated cell death on expression of the fungal avirulence gene *Avr9* in tomato seedlings carrying the disease-resistance gene *Cf-9*. *Proceedings of the National Academy of Sciences of the United States of America*, 24, 10445–10449.
- Han, Y., Song, L., Peng, C., Liu, X., Liu, L., Zhang, Y. et al. (2019) A *Magnaporthe* chitinase interacts with a rice jacalin-related lectin to promote host colonization. *Plant Physiology*, 179, 1416–1430.
- Jashni, M.K., Mehrabi, R., Collemare, J., Mesarich, C.H. & de Wit, P.J.G.M. (2015) The battle in the apoplast: further insights into the roles of proteases and their inhibitors in plant–pathogen interactions. *Frontiers in Plant Science*, 6, 584.
- de Jonge, R., van Esse, H.P., Kombrink, A., Shinya, T., Desaki, Y., Bours, R. et al. (2010) Conserved fungal LysM effector Ecp6 prevents chitin-triggered immunity in plants. *Science*, 329, 953–955.
- Jones, J.D.G. & Dangl, J.L. (2006) The plant immune system. *Nature*, 444, 323–329.
- Kamoun, S. (2006) A catalogue of the effector secretome of plant pathogenic oomycetes. *Annual Review of Phytopathology*, 44, 41–60.
- Kamoun, S., van West, P., de Jong, A.J., de Groot, K.E., Vleeshouwers, V.G.A.A. & Govers, F. (1997) A gene encoding a protein elicitor of *Phytophthora infestans* is down-regulated during infection of potato. *Molecular Plant-Microbe Interactions*, 10, 13–20.
- Kobayashi, M., Hiraka, Y., Abe, A., Yaegashi, H., Natsume, S., Kikuchi, H. et al. (2017) Genome analysis of the foxtail millet pathogen *Sclerospora graminicola* reveals the complex effector repertoire of graminicolous downy mildews. *BMC Genomics*, 18, 897.
- Lamour, K. & Kamoun, S. (2009) *Oomycete genetics and genomics: diversity, interactions, and research tools*. New Jersey: John Wiley & Sons.
- Lenarčič, T., Albert, I., Böhm, H., Hodnik, V., Pirc, K., Zavec, A.B. et al. (2017) Eudicot plant-specific sphingolipids determine host selectivity of microbial NLP cytolysins. *Science*, 358, 1431–1434.
- Maqbool, A., Saitoh, H., Franceschetti, M., Stevenson, C.E.M., Uemura, A., Kanzaki, H. et al. (2015) Structural basis of pathogen recognition by an integrated HMA domain in a plant NLR immune receptor. *eLife*, 4, e08709.
- Marshall, R., Kombrink, A., Motteram, J., Loza-Reyes, E., Lucas, J., Hammond-Kosack, K.E. et al. (2011) Analysis of two in planta expressed LysM effector homologs from the fungus *Mycosphaerella graminicola* reveals novel functional properties and varying contributions to virulence on wheat. *Plant Physiology*, 156, 756–769.
- Mentlak, T.A., Kombrink, A., Shinya, T., Ryder, L.S., Otomo, I., Saitoh, H. et al. (2012) Effector-mediated suppression of chitin-triggered immunity by *Magnaporthe oryzae* is necessary for rice blast disease. *The Plant Cell*, 24, 322–335.
- Morgan, W. & Kamoun, S. (2007) RXLR effectors of plant pathogenic oomycetes. *Current Opinion in Microbiology*, 10, 332–338.
- Oome, S. & Van den Ackerveken, G. (2014) Comparative and functional analysis of the widely occurring family of Nep1-like proteins. *Molecular Plant-Microbe Interactions*, 27, 1081–1094.
- Ottmann, C., Luberaacki, B., Küfner, I., Koch, W., Brunner, F., Weyand, M. et al. (2009) A common toxin fold mediates microbial attack and plant defense. *Proceedings of the National Academy of Sciences of the United States of America*, 106, 10359–10364.
- Raffaele, S., Win, J., Cano, L.M. & Kamoun, S. (2010) Analyses of genome architecture and gene expression reveal novel candidate virulence factors in the secretome of *Phytophthora infestans*. *BMC Genomics*, 11, 637.
- Shibata, Y., Kawakita, K. & Takemoto, D. (2010) Age-related resistance of *Nicotiana benthamiana* against hemibiotrophic pathogen *Phytophthora infestans* requires both ethylene- and salicylic acid-mediated signaling pathways. *Molecular Plant-Microbe Interactions*, 23, 1130–1142.
- Takahashi, M., Yoshioka, K., Imai, T., Miyoshi, Y., Nakano, Y., Yoshida, K. et al. (2013) Degradation and synthesis of β -glucans by a *Magnaporthe oryzae* endotransglucosylase, a member of the glycoside hydrolase 7 family. *Journal of Biological Chemistry*, 288, 13821–13830.
- Thines, M. & Kamoun, S. (2010) Oomycete–plant coevolution: recent advances and future prospects. *Current Opinion in Plant Biology*, 13, 427–433.
- Torto, T.A., Li, S., Styer, A., Huitema, E., Testa, A., Gow, N.A.R. et al. (2003) EST mining and functional expression assays identify extracellular effector proteins from the plant pathogen *Phytophthora*. *Genome Research*, 13, 1675–1685.
- Wang, Y., Tyler, B.M. & Wang, Y. (2019) Defense and counterdefense during plant-pathogenic oomycete infection. *Annual Review of Microbiology*, 73, 667–696.
- Wang, Y. & Wang, Y. (2018) Trick or treat: microbial pathogens evolved apoplastic effectors modulating plant susceptibility to infection. *Molecular Plant-Microbe Interactions*, 31, 6–12.
- Wawra, S., Fesel, P., Widmer, H., Timm, M., Seibel, J., Leson, L. et al. (2016) The fungal-specific β -glucan-binding lectin FGB1 alters cell-wall composition and suppresses glucan-triggered immunity in plants. *Nature Communications*, 7, 13188.
- Weidenbach, D., Esch, L., Möller, C., Hensel, G., Kumlehn, J., Höfle, C. et al. (2016) Polarized defense against fungal pathogens is mediated by the Jacalin-related lectin domain of modular *Poaceae*-specific proteins. *Molecular Plant*, 9, 514–527.
- Win, J., Krasileva, K.V., Kamoun, S., Shirasu, K., Staskawicz, B.J. & Banfield, M.J. (2012) Sequence divergent RXLR effectors share a structural fold conserved across plant pathogenic oomycete species. *PLoS Pathogens*, 8, e1002400.
- Xiang, Y., Song, M., Wei, Z., Tong, J., Zhang, L., Xiao, L. et al. (2011) A jacalin-related lectin-like gene in wheat is a component of the plant defence system. *Journal of Experimental Botany*, 62, 5471–5483.

SUPPORTING INFORMATION

Additional supporting information may be found in the online version of the article at the publisher's website.

How to cite this article: Kobayashi, M., Utsushi, H., Fujisaki, K., Takeda, T., Yamashita, T. & Terauchi, R. (2022) A jacalin-like lectin domain-containing protein of *Sclerospora graminicola* acts as an apoplastic virulence effector in plant–oomycete interactions. *Molecular Plant Pathology*, 23, 845–854. <https://doi.org/10.1111/mpp.13197>